The Seasonal Cycle over the Tropical Pacific in Coupled Ocean–Atmosphere General Circulation Models

C. R. MECHOSO,* A. W. ROBERTSON,* N. BARTH,† M. K. DAVEY,# P. DELECLUSE,@ P. R. GENT,& S. INESON,# B. KIRTMAN,** M. LATIF,†† H. LE TREUT,## T. NAGAI,@@ J. D. NEELIN,* S. G. H. PHILANDER,&& J. POLCHER,## P. S. SCHOPF,*** T. STOCKDALE,††† M. J. SUAREZ,*** L. TERRAY,### O. THUAL,### AND J. J. TRIBBIA&

*Department of Atmospheric Sciences, University of California, Los Angeles, Los Angeles, California
†Scripps Institution of Oceanography, La Jolla, California
#Hadley Centre for Climate Prediction and Research, Meteorological Office, Bracknell, United Kingdom
@LODYC, Universite de Pierre et Marie Curie, Paris, France
&National Center for Atmospheric Research, Boulder, Colorado
**Center for Ocean–Land–Atmosphere Studies, Calverton, Maryland
††Max Planck Institut für Meteorologie, Hamburg, Germany
##Laboratoire de Meteorologie Dynamique du CNRS, Paris, France
@@Tokyo Institute of Technology, Ookayama, Meguro, Tokyo, Japan
&&Geophysical Fluid Dynamics Laboratory, Princeton, New Jersey
***NASA/Goddard Space Flight Center, Greenbelt, Maryland
†††European Centre for Medium-Range Weather Forecasts, Reading, United Kingdom
###CERFACS, Toulouse, France

(Manuscript received 26 September 1994, in final form 26 January 1995)

ABSTRACT

The seasonal cycle over the tropical Pacific simulated by 11 coupled ocean–atmosphere general circulation models (GCMs) is examined. Each model consists of a high-resolution ocean GCM of either the tropical Pacific or near-global oceans coupled to a moderate- or high-resolution atmospheric GCM, without the use of flux correction. The seasonal behavior of sea surface temperature (SST) and eastern Pacific rainfall is presented for each model.

The results show that current state-of-the-art coupled GCMs share important successes and troublesome systematic errors. All 11 models are able to simulate the mean zonal gradient in SST at the equator over the central Pacific. The simulated equatorial cold tongue generally tends to be too strong, too narrow, and extend too far west. SSTs are generally too warm in a broad region west of Peru and in a band near 10°S. This is accompanied in some models by a double intertropical convergence zone (ITCZ) straddling the equator over the eastern Pacific, and in others by an ITCZ that migrates across the equator with the seasons; neither behavior is realistic. There is considerable spread in the simulated seasonal cycles of equatorial SST in the eastern Pacific. Some simulations do capture the annual harmonic quite realistically, although the seasonal cold tongue tends to appear prematurely. Others overestimate the amplitude of the semiannual harmonic. Nonetheless, the results constitute a marked improvement over the simulations of only a few years ago when serious climate drift was still widespread and simulated zonal gradients of SST along the equator were often very weak.

1. Introduction

a. Background

Intense research effort is increasingly being focused on the ambitious task of simulating the climate system using coupled ocean–atmosphere general circulation models (CGCMs). Progress has been very rapid, so that there are now over a dozen CGCMs with comparably high resolution and sophistication; this is many more than at the time of the recent review of Neelin et al. (1992). This progress has been encouraged by the perception that successful simulation and prediction of aspects of the El Niño–Southern Oscillation phenomenon (ENSO) using CGCMs is within our grasp. Some success has already been achieved by simplified models of the coupled ocean–atmosphere system (Cane et al. 1986; Zebiak and Cane 1987; Schopf and Suarez 1988), as well as by one or two CGCMs (Nagai et al. 1992; Latif et al. 1994a); see the recent review of ENSO prediction studies by Latif et al. (1994b).

There is now widespread agreement that ENSO involves coupled oscillations of the tropical atmosphere–ocean system and that these oscillations are sensitive to the mean state of the system (Zebiak and Cane 1987;

Corresponding author address: Dr. A. W. Robertson, Department of Atmospheric Sciences, University of California, Los Angeles, 405 Hilgard Avenue, Los Angeles, CA 90095-1565.

Schopf and Suarez 1988; Suarez and Schopf 1988; Battisti and Hirst 1989; Neelin 1991). Several factors point to the important role played by the seasonal cycle in ENSO. Most fundamentally, the extremes of El Niño usually occur in northern winter, so that ENSO appears "phase-locked" to the seasonal cycle. A seasonal dependence in the predictability of ENSO is now well established (see, e.g., Latif et al. 1994b), but the processes responsible for it are not fully understood. Third, recent theoretical work suggests that the seasonal cycle plays a crucial role in determining the spectrum of ENSO and may contribute to its aperiodic nature (Jin et al. 1994; Tziperman et al. 1994). Only coupled general circulation models attempt to simulate all the elements that interact to determine climate. The intimate dependency of anomalies on the mean state and seasonal cycle, therefore, presents a major challenge to CGCM modelers, since in order to simulate interannual anomalies *realistically,* the model must also be able to simulate the mean state and seasonal cycle. While anomaly models can confine themselves to simulating the more or less adiabatic east–west redistribution of heat across the Pacific in the oceanic mixed layer along the equator, coupled GCMs must be able to model the large component of the seasonal cycle that is meridionally antisymmetric about the equator, as well as the diabatic processes associated with the thermodynamic equilibrium associated with the mean state. These are just the components of atmospheric modeling that present the greatest challenges. To date, the seasonal cycle over the tropical Pacific has indeed proven difficult to simulate.

This paper is preceded by the analyses of the tropical simulations of 17 coupled GCMs by Neelin et al. (1992). Each one of these models had one component with sufficient complexity to be called a GCM. The ocean domains ranged from the tropical Pacific basin to the near-global oceans, with the latter models having lower resolution in general. The results of these analyses were recently updated in the review by Neelin et al. (1994). Of the 10 models with a freely evolving "mean" state (i.e., without flux correction or a prescribed climatology), most exhibited serious climate drift: either a slow drift away from climatology or a relatively fast adjustment leading to a state very different from normal climatology. In particular, many of the model simulations had weak zonal gradients along the equator. The models exhibited a variety of interannual behaviors, from weak variability to interannual variability, with zonally propagating or standing SST anomalies. Surprisingly, the presence of climate drift appeared to bear little relationship to the existence of significant interannual variability, provided the cold tongue was resolved in the eastern basin.

b. *Our study*

The development of coupled GCMs for simulation of tropical climate anomalies has recently reached the stage where there are now about a dozen models of comparable sophistication that have been integrated for about a simulated decade or more. It is thus now possible to make a meaningful assessment of the successes and failures in a relatively homogeneous set of model experiments. While a decade generally suffices to characterize the mean state and seasonal cycle in the Tropics, it is too short for a meaningful intercomparison of interannual variability. Nevertheless, the analysis of the seasonal cycle is a necessary first step in coupled model validation, even from the point of view of interannual variability as discussed above.

It is clear from the outset that the many differences in model construction preclude a simple categorization of model behavior as a function of model configuration. Several models do share common components—even the entire ocean in several cases—engendering the hope that common threads of behavior may lead us to isolate a particular problem. However, there are dramatic examples of the sensitivity of the coupled system to subtle changes in parameterization of selected physical processes, with the rest of the model held fixed (e.g., Ma et al. 1994). In the pragmatic task of producing a reasonably realistic simulated climate with a coupled GCM, model "tuning"—through choice of parameterization scheme and parameters—is an unavoidable step in coupled GCM development, with the inevitable consequence of some degree of compensation of errors.

This study examines the behavior of an ensemble of 11 high-resolution coupled GCMs that do not use flux correction. High-resolution ocean models can resolve the equatorial ocean wave modes, which are important components of the coupled modes characterizing observed ENSO events. Our methodology is based on defining a "climate space" in terms of a few fundamental characteristics of the climate of the atmosphere–ocean system over the tropical Pacific and charting the behavior of our ensemble of 11 models. Selected figures from each of the model simulations, together with observed estimates, are plotted in a unified format. The purpose of this work is not to rank models according to their success or failure in the simulation of the seasonal cycle. Rather, we attempt to discuss the errors common to the models in order to stimulate modeling work directed toward correcting these deficiencies, both in the simulation of the seasonal cycle and, accordingly, interannual variability.

In the interests of selecting the most representative results, we concentrate on the sea surface temperature (SST) as a sensitive indicator of the state of the coupled system. First, we consider the annual mean east–west gradient of SST along the equator, which plays an important role in air–sea interaction, as well as being itself partly a product of it (Dijkstra and Neelin 1994). Next, we focus on the pronounced annual cycle in equatorial SST over the eastern part of the basin, which

contrasts starkly with the very weak seasonal variation in SST west of 150°W.

The seasonal cycle along the equator can be understood only in the context of the coupled ocean–atmosphere system in the Tropics as a whole. Latitudinal displacements of the trade-wind belts are felt at the equator and are intimately related to the annual cycle of the equatorial cold tongue. The persistence of the intertropical convergence zone (ITCZ) north of the equator over the eastern Pacific is one of the most remarkable features of the climate in the region. This persistence has been interpreted in terms of the effects of continental asymmetries on upwelling, stratus cover, and convergence zones (Mitchell and Wallace 1992), as well as coupled feedbacks, in particular an evaporation feedback mechanism (Xie and Philander 1994). To address the models' success in simulating the seasonal cycle throughout the tropical Pacific, we display spatial maps of SST for April and October. To track meridional seasonal displacements of the ITCZ, the final figure shows the seasonal cycle in rainfall over the eastern Pacific with latitude. Taken together, these figures enable the position and intensity of the ITCZ to be interpreted in terms of the underlying SST, from which the general character of upwelling, mixing, and evaporation can often be anticipated. The latter are important determinants of SST over the eastern equatorial Pacific where the thermocline shoals.

All contributors are listed as authors. The two lead authors have assembled the model results and written the text. Any errors or omissions remain the responsibility of the lead authors. Section 2 summarizes the models, the results are presented in section 3, and the paper concludes with a discussion in section 4.

2. Model descriptions

A summary of each of the models is given in Table 1, together with a reference where details of the respective models can be found. Regarding the atmospheric components (AGCMs), six are spectral and five are gridpoint models; none of the coupled models share a common atmospheric component. Horizontal resolution ranges from about T21 to T42, or a grid size of about 6° to 3°. In the vertical, the number of layers ranges from 5 to 30, although note that the CERFACS model (Arpege) has high resolution in the stratosphere. Only the models' cumulus parameterization schemes are included in Table 1. For details of these and the parameterizations of radiation, boundary layer, and other physical processes, the reader is referred to the references in Table 1.

The GFDL (Geophysics Fluid Dynamics Laboratory; Bryan 1969; Cox 1984) OGCM is common to four of the coupled models in different configurations, while the HOPE (Hamburg Ocean Primitive Equations Model; Latif et al. 1994a) and OPA (Andrich et al. 1988) OGCMs are each used identically in two

TABLE 1. Model descriptions. Spatial resolution is given as the latitude–longitude grid size or "T" or "R" for triangular or rhomboidal spectral truncation, respectively. The number of model levels/layers is denoted by "L." Key to convection schemes: MF—mass flux, SC—shallow convection, MCA—moist convective adjustment, MCC—moisture convergence closure, AS—Arakawa–Schubert, DD—downdrafts. Key to ocean mixing: TKE—turbulent kinetic energy closure, Ri—Richardson number dependent, ML—explicit mixed layer. See text for further details.

Model	CERFACS	COLA	EC	GFDL	GSFC	LMD/LODYC	MPI	MRI	NCAR	UCLA	UKMO
AGCM:	Arpege	COLA	EC	GFDL	Aries	LMD	ECHAM	MRI	CCM2	UCLA	UKMO
Resolution:	T42	R15	T21	R30	5° × 4°	64 × 50 pts.	T42	5° × 4°	T42	5° × 4°	3.75° × 2.5°
	L30	L18	L19	L9	L13	L11	L19	L5	L12	L9	L19
Convection scheme:	MF + SC	MCC + SC	MF + SC	MCA	relaxed AS	MCC + MCA	MF + SC	AS	MF	AS	MF + DD
OGCM:	OPA	GFDL	HOPE	GFDL	Poseidon	OPA	HOPE	MRI	Gent/Cane	GFDL	GFDL
	T-Pacific	global	global	global	global	T-Pacific	global	Ind.–Pac.	T-Pacific	T-Pacific	T-Pacific
	40°S–48°N	70°S–65°N	60°S–60°N	50°S–50°N	90°S–72°N	40°S–48°N	60°S–60°N	40°S–30°N	20°S–20°N	30°S–50°N	30°S–30°N
Resolution:	0.75° × 1/3°–1.5°	1.5° × 0.5°–1.5°	2.8° × 0.5°–2.8°	1° × 1/3°–3°	1.25° × 2/3°	0.75° × 1/3°–1.5°	2.8° × 0.5°–2.8°	2° × 1°	1° × 1/4°–1°	1° × 1/3°–3°	1.5° × 1/3°–1°
	L28	L20	L20	L27	isopyc. L8	L28	L20	L20	L7	L27	L16
Ocean mixing:	1.5 TKE	Ri	Ri + ML	Ri	Ri + ML	1.5 TKE	Ri + ML	2.0 TKE	Ri	2.5 TKE	Ri + ML
Reference:	Terray et al. (1994)	Schneider & Kinter (1994)	Stockdale et al. (1994)			Barth & Polcher (1994)	Latif et al. (1994a)	Nagai et al. (1994)	Gent & Tribbia (1993)	Robertson et al. (1995a)	Ineson & Davey (1994)

CERFACS: Centre Européende Recherche et de Formation Avancée en Calcul Scientifique
COLA: Center for Ocean–Land–Atmosphere Studies
EC: European Centre for Medium-Range Weather Forecasts
GFDL: Geophysical Fluid Dynamics Laboratory
GSFC: Goddard Space Flight Center
LMD: Laboratoire de Meteorologie Dynamique
MPI: Max-Planck-Institut für Meteorologie
MRI: Meteorological Research Institute, Japan
NCAR: National Center for Atmospheric Research
UCLA: University of California, Los Angeles
UKMO: United Kingdom Meteorological Office

CGCMs. Of the 11 models, 5 have an interactive ocean confined to the tropical Pacific basin (T-Pacific) and 1 (MRI) includes the Indian Ocean (Ind–Pac). The remaining 5 have near-"global" OGCMs whose interactive–ocean extents are given in Table 1. Only the GSFC model's ocean extends to Antarctica in the south and includes all but the Arctic Ocean in the north. The HOPE model (EC and MPI) is actually global in extent, but SST and surface salinity are relaxed to climatological values poleward of 60°. Although no model uses flux correction to eliminate climate drift, the models whose ocean domain is limited to the Tropics include relaxation to climatological conditions close to the boundaries of our region of interest. Furthermore, horizontal resolution is somewhat higher in the tropical Pacific basin models, so we might expect, a priori, their performance to be better. Our ensemble includes one isopycnic (GSFC) and one reduced gravity model (NCAR). Ocean mixing is parameterized using a Richardson number–dependent scheme in seven of the models, three of which include an explicit mixed layer. The remaining four models use turbulence closure schemes, involving prognostic equations for turbulence quantities. The effects of solar radiation on the thermal state of the ocean below the first model layer is considered in all except the NCAR and UCLA models.

All models were initialized to some (partially) spunup ocean state, except for COLA, GFDL, MPI, and UCLA, which were integrated from an ocean at rest with climatological distributions of monthly mean temperature and salinity. The climatologies shown are time averages over about 10 years, except GFDL (2 years), LMD/LODYC (5 "normal" years), MPI and UKMO (25 years), and GSFC (40 years). The GFDL model has very weak interannual variability. The averaging periods generally commence after some years of integration, especially in the cases of the models started from an ocean at rest. No appreciable drift was noted during the averaging period in any of the models, except GSFC where the climatology spans the latter 40 years of a 60-yr integration. In the GSFC model—which is the most global in extent, see above—tropical SSTs cool by about 1°C during the first 20 years of the averaging period and warm by a similar amount in the last 20 years.

3. Results

a. Annual-mean SST on the equator

Figure 1 illustrates the annual-mean SST based on COADS (Comprehensive Ocean–Atmosphere Data Set) data along the equator (Oberhuber 1988; thick line), together with the model simulations (all are averages 2°S–2°N). The gradient of the curve obtained with observed data is almost constant across much of the basin with a magnitude of about 0.4°C per 10° longitude. Toward the edges of the basin the SST gradient

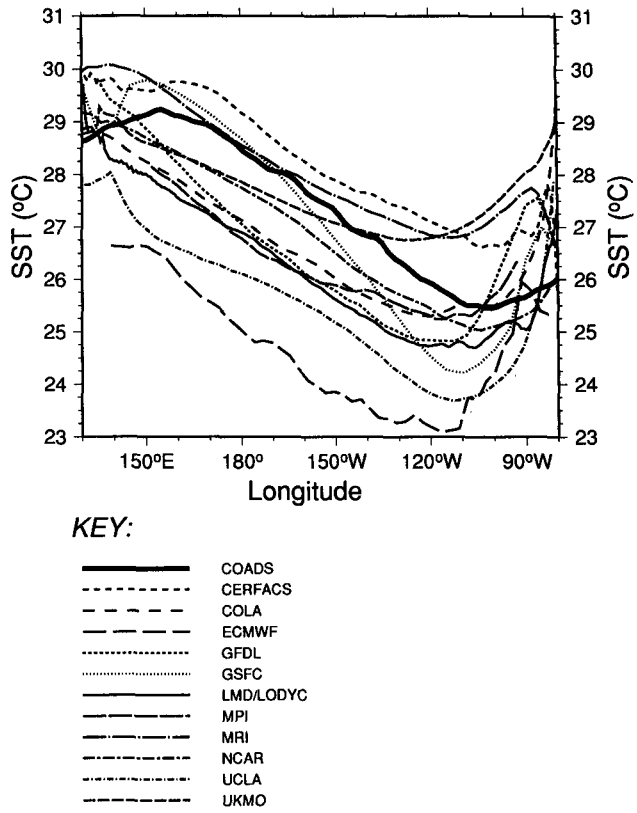

FIG. 1. Annual mean SST along the equator averaged between 2°S and 2°N.

decreases and changes sign, with the SST variation in the west almost mirroring that in the east. The simplicity and smoothness of the variation along the equator is striking.

Almost all the coupled-model simulations succeed in approximating the east–west gradient in SST across the basin. This is a clear improvement over the situation at the time of Neelin et al. (1992). However, almost all models produce a pattern more complex than the observed, especially near the coasts. The simulations are most successful over the longitudinal range where the observed gradient is almost constant (160°E–120°W). Here, simulated magnitudes are within 2°C of observed with the preponderance colder, excepting UCLA and EC, which are 2°–3°C too cold. We note that the "blended" SSTs of NMC's Climate Analysis Center (Reynolds 1988) for 1982–93 are actually colder by up to 1°C in the eastern Pacific at the equator than the COADS data in Fig. 1 (high-resolution satellite measurements are included). Simulated gradients are also generally reasonable over the central Pacific—if slightly underestimated and less uniform than observed—with the exception of the GSFC and UKMO models, where the gradient in equatorial SST is significantly over- and underestimated respectively.

TABLE 2. Annual mean SST along the equator in central Pacific in terms of magnitude and gradient between 160°E and 120°W (Fig. 1).

	Magnitude	
Gradient	Underestimated (1°–3°C)	Realistic (±1°C)
Underestimated		UKMO
Realistic	COLA	CERFACS
	EC	MRI
	GFDL	NCAR
	LMD/LODYC	
	MPI	
	UCLA	
Overestimated		GSFC

It is toward the coasts that the mean equatorial SST is most poorly simulated. East of 90°W simulated SST is overestimated by up to 3°C, although some models exhibit a narrow strip along the coast of Peru where SST decreases to more realistic values. The zonal gradients of simulated SST are much too large east of 110°W in most cases, as the corresponding values go from being underestimated to the west and overestimated to the east; the upwelling tongue tends to be displaced westward of its observed position. Only the NCAR model produces a realistic simulation near the eastern boundary. The annual mean SST along the equator is better simulated toward Indonesia than off the coast of Peru, but the SST produced by the CGCMs generally exceeds observed values west of 150°E and has a zonal variation that is somewhat erratic in many models. This may be related to the OGCM boundary conditions. The main features of the simulations of annual-mean equatorial SST are summarized in Table 2.

b. The seasonal cycle of equatorial SST

Figure 2 shows the seasonal cycle in the deviations of SST at the equator about the annual mean (i.e., Fig. 1), again for the COADS data and each model simulation. The variation in observed SST is dominated by the annual harmonic that peaks at about 100°W, with the warm phase in April stronger than the cold phase in September–October.

The bulk of seasonal variation in equatorial SST is realistically located over the eastern Pacific in all models, although deviations are concentrated too close to the coast in some models. The seasonal cycle is very weak in three of the models, and only four obtain a reasonably realistic annual cycle in both phase and amplitude (Table 3). Simulated SST is correctly dominated by the annual harmonic in most cases. The semiannual harmonic is overpronounced in some simulations (GSFC and MRI) and dominates in the GFDL simulation. No model captures the relative amplitudes

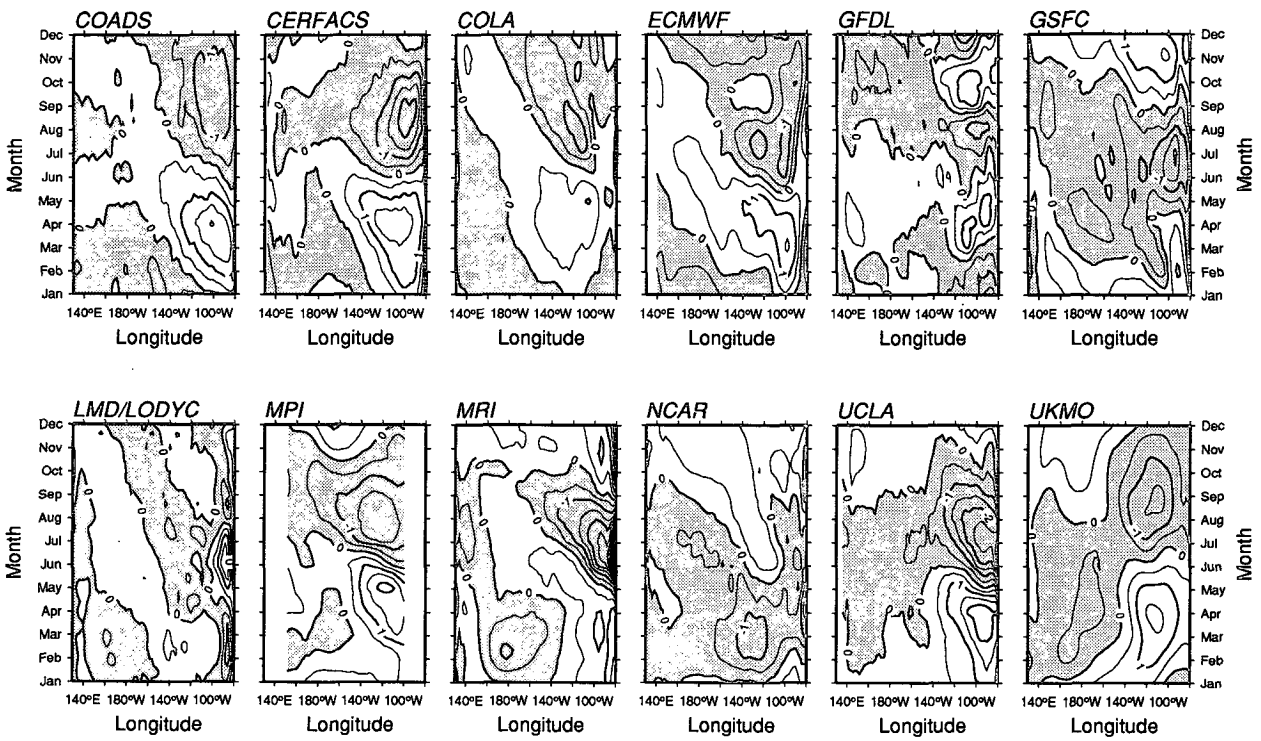

FIG. 2. The seasonal cycle in equatorial SST (2°S–2°N) in terms of deviations from the respective annual mean given in Fig. 1. Contour interval is 0.5°C, and negative anomalies are stippled.

TABLE 3. Phase and amplitude of the annual cycle of SST at the equator in the eastern Pacific (Fig. 2).

	Phase		
Magnitude	Realistic	Cold phase premature	Poor
Little annual cycle			LMD/LODYC GFDL (semiannual cycle)
Underestimated	COLA		NCAR
Realistic	CERFACS	EC	
	MPI	GSFC	
	UKMO	MRI	
Overestimated		UCLA	

and phases of the two leading harmonics sufficiently well to reproduce the observed asymmetry in amplitude in the seasonal cycle that peaks in April. Where the seasonal cycle has realistic amplitude, the timing of the warm phase of the cycle in April is more successfully captured than that of the cold phase, which arrives too early and decays too quickly. The transition to the cold phase is clearly much more rapid in most of the models than in reality. The observed tendency for the seasonal cycle in SST to propagate westward is captured in many of the models, although interestingly, there appears to be little correspondence between this success and a model's ability to simulate other aspects of the seasonal cold tongue.

Figure 2 is a graphic example of how very different results can be obtained in coupled GCMs even if the oceanic component is identical, as it is in CERFACS and LMD/LODYC and in EC and MPI.

c. *Composite maps of SST*

In order to investigate further the seasonality of tropical SST, we examine maps of SST for the months of April and October in Figs. 3 and 4, respectively, plotted on a 2° latitude–longitude grid; these are the months of seasonal extrema of observed SST at the equator (Fig. 2). In the COADS data, the seasonal cycle is characterized over the western Pacific by the meridional migration of the warm pool with the seasons and by the equatorial extension of the cold tongue over the eastern Pacific, which reaches its maximum extent in October.

In April, there is only a hint of a cold tongue on the equator, concurrent with the seasonal minimum in the strength of the southeast trades (e.g., Robertson et al. 1995a). Most models, however, produce a narrow tongue of cold water along the equator in April. Only the CERFACS and UKMO models simulate the disappearance of the equatorial cold tongue in April, and consistently, they are among those that have a realistic seasonal cycle in SST at the equator (Fig. 2, Table 3). Aside from the spurious equatorial cold tongue, another general problem in the simulations in April is the degree of meridional symmetry in the eastern Pacific, where a narrow tongue of warm water occurs south of the equator. Meridional gradients of SST are generally substantially overestimated throughout the Tropics.

In October, the observed distribution of SST has a strong cold tongue in the southeast and a large warm pool in the west. Every model simulates these two features to some extent, although note that October is a favorable month to validate for the models whose seasonal cold tongue is overintense but premature (Fig. 2). As in April, SSTs are generally overestimated over the eastern Pacific south of the equator. This is found to be associated with overestimated solar insolation (not shown), suggesting that there are deficiencies in the simulation of low-level stratus clouds. Only the GSFC model obtains a local minimum in solar isolation off the coast of Peru as observed, and this is consistent with somewhat colder SSTs. Even in October, the warm pool extends too far east near 10°S in every simulation. This feature, together with the tendency for the cold tongue to extend too far west along the equator, bisecting the warm pool in most models, makes simulated meridional gradients too large, while reducing zonal gradients. The surface temperature of the west Pacific warm pool (29°–30°C) is well simulated by most models, although—as in April—its meridional extent is seriously underestimated in several cases. The local SST maximum off the coast of Mexico appears in some simulations but not others.

d. *Precipitation over the eastern Pacific*

Figures 3 and 4 highlight the narrowness of the cold tongue in the eastern Pacific in most models, with unrealistically warm SSTs south of the equator. To see to what extent convection is taking place south of the equator in the eastern Pacific, and to investigate its seasonality, Hovmöller diagrams of precipitation averaged from 100° to 150°W are plotted in Fig. 5. Rainfall estimated from observed OLR for 1986–89 (Janowiak and Arkin 1991) is largely confined to an ITCZ located persistently between 5° and 15°N. Seasonal variation in latitude is small, with the ITCZ reaching its northernmost position around September and its southernmost in March–April, when it dips almost to the equator. According to the OLR proxy, maximum rainfall occurs in northern summer, coincident with the band of high SSTs north of the equator (Fig. 4). There is a pronounced minimum in February–March that is less meridionally confined, again consistent with the underlying SSTs.

Simulated rainfall maxima have realistic magnitudes, but their location and seasonality are generally poor. Precipitation is on average severely overestimated south of the equator over the eastern Pacific in all models, except in the LMD/LODYC model, which

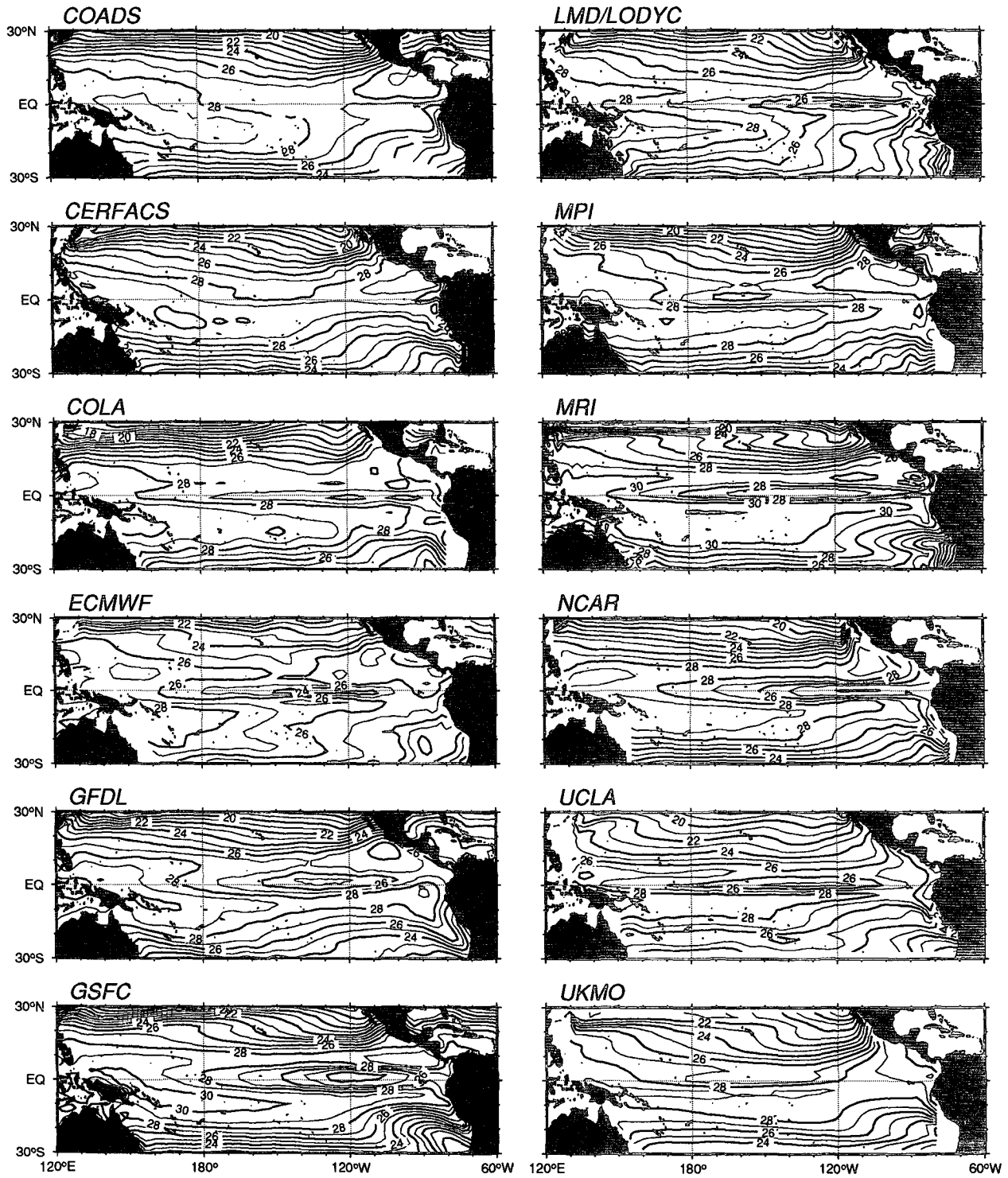

FIG. 3. Maps of mean SST for April. Contours are every 1°C.

has almost no seasonal cycle in SST (Figs. 2–4). Comparing with the distributions of SST in Figs. 3 and 4 reveals the importance of SST in determining the location of precipitation in the simulations. Model behavior falls roughly into two categories: (i) simulations that produce a rather persistent double ITCZ, and (ii)

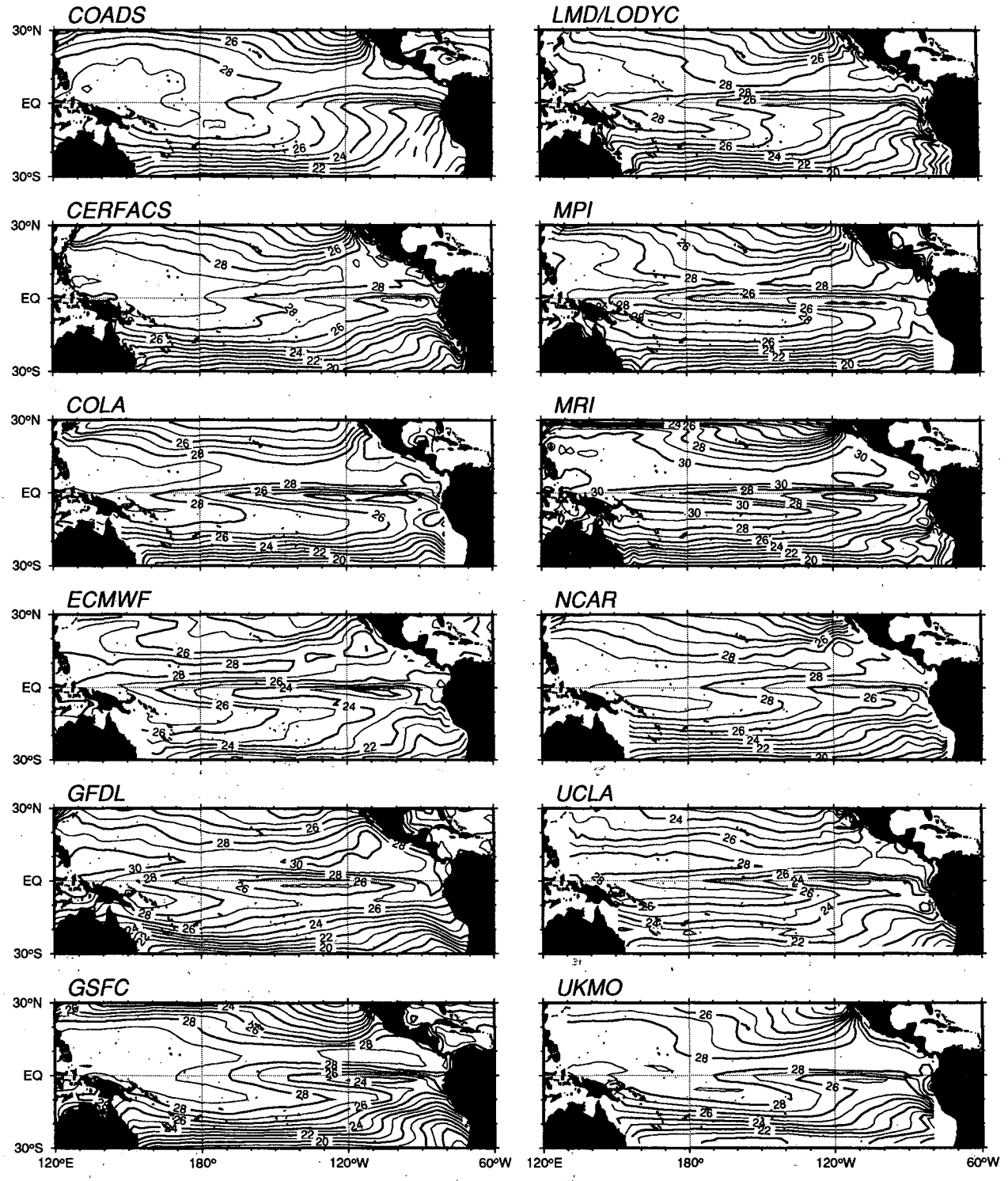

FIG. 4. Maps of mean SST for October. Contours are every 1°C.

simulations in which the ITCZ shows a pronounced north–south seasonal migration (see Table 4). Neither of these behaviors is realistic, although the OLR data do show a limited meridional migration, and there is a hint of a double ITCZ in March–April; the latter is also documented by Walliser and Gautier (1993).

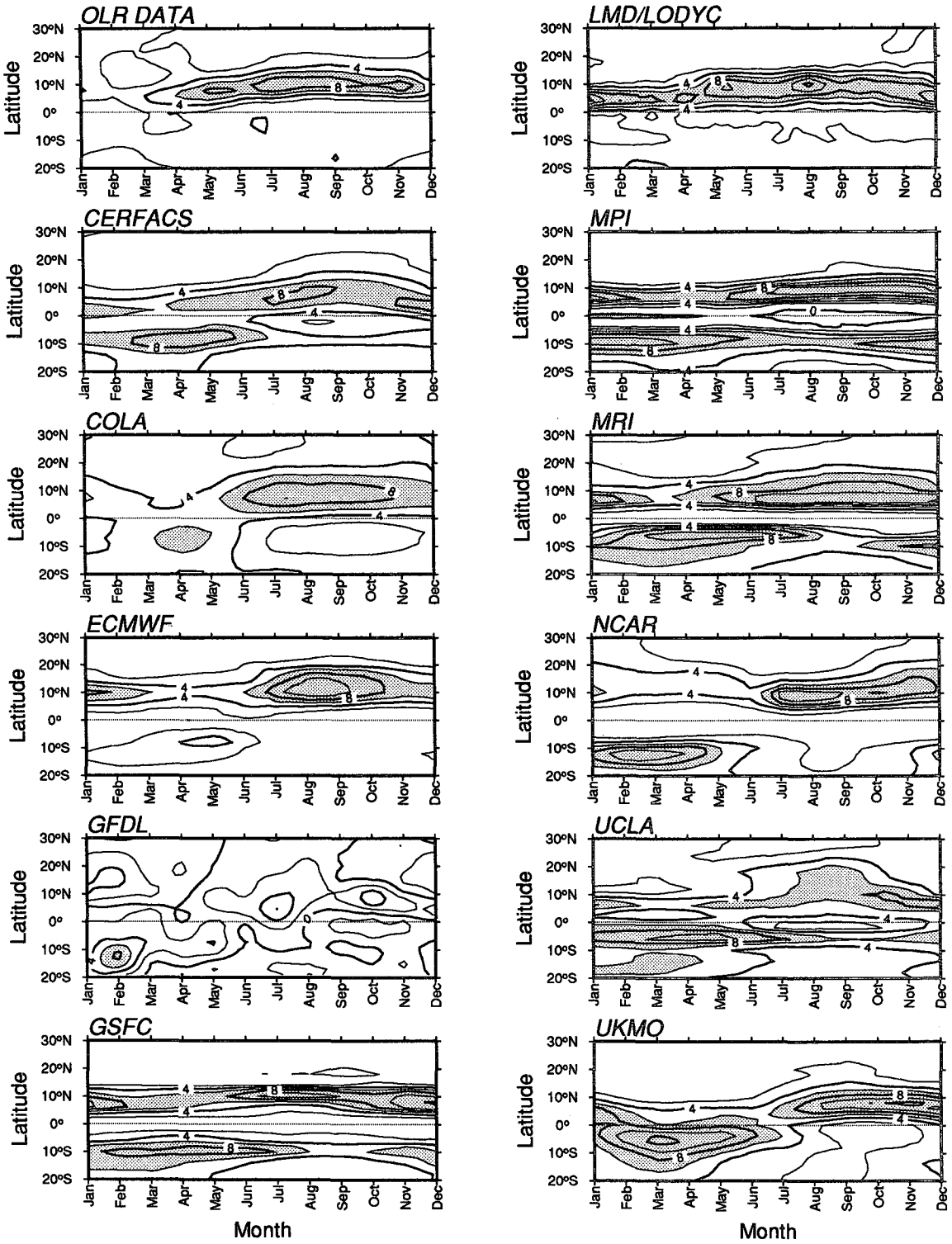

FIG. 5. The seasonal cycle in precipitation over the eastern Pacific (averaged between 150° and 100°W) plotted against latitude. For the GFDL model, precipitation minus evaporation is plotted. The observed estimate is derived from cloud-top temperatures for 1986–89 (Janowiak and Arkin 1991). Contour interval is 2 mm day^{-1}, with values greater than 6 mm day^{-1} stippled.

TABLE 4. Seasonal cycle of the ITCZ in terms of precipitation averaged over the eastern Pacific between 150° and 100°W (Fig. 5).

Single ITCZ	LMD/LODYC
Double ITCZ	GSFC, MPI, MRI, UCLA
Migrating ITCZ	CERFACS, COLA, EC, GFDL, NCAR, UKMO

4. Discussion

We have analyzed the main features of the tropical Pacific climate simulated by 11 coupled GCMs. Each of the models considered here consists of a high-resolution ocean GCM of the tropical Pacific or near-global oceans, coupled to a moderate or high-resolution atmospheric GCM, without the use of flux correction. The models are summarized in Table 1, and our principal results are shown in Tables 2–4.

The central aim of this paper has been to identify common strengths and deficiencies in the mean state and seasonal cycle over the tropical Pacific simulated by coupled GCMs. The underlying hope is to link such shared behavioral traits with aspects of common model characteristics, such as resolution, physical parameterizations, etc. Some important questions arise. Why is the simulated cold tongue often too strong, narrow, overelongated, perennial, and premature in its onset? Why are SSTs overestimated west of Peru and in a band near 10°S in the east and central Pacific? Why is it that some models have a perennial double ITCZ associated with this, while in others the ITCZ migrates across the equator with the seasons? Why is the semiannual harmonic often overestimated? Do these deficiencies have their roots in the atmospheric or oceanic components of the models, or in the coupling between them?

a. The annual mean state

The models have several common deficiencies in reproducing the observed annual-average state and seasonal cycle. For the annual average state, we note three rough categories for discussing problematic areas: (i) the structure of SST along the equator involving the equatorial cold tongue and the transition to the western Pacific warm pool, (ii) the north–south structure in the eastern Pacific, and (iii) the meridional extent of the warm pool.

In the first category, the structure of the annual mean SST along the equator shows considerable variation among the GCMs. It is often simulated as having complex structure near the coasts, in contrast to the simplicity of the observed structure, which has a strong gradient through the central basin, with a broad minimum around 100°–110°W and only a slight relative warming near the Peruvian coast. The models do succeed in producing SST gradients in midbasin that are comparable to or exceed the observed (with the exception of UKMO); SST values in most cases are 1°–3°C colder than observed in the central Pacific. This occurs despite equatorial wind stress values that are concurrently underestimated—generally by about a factor of 2 in the mean, see, for example, Nagai et al. (1995) and Robertson et al. (1995a)—and thus would be expected to yield smaller thermocline slopes and less equatorial upwelling than observed winds. However, contemporary OGCMs (except OPA) tend to produce stronger than observed cold tongues when forced with observed wind stress (Stockdale et al. 1993), and this apparently compensates for the weak stress in the coupled simulations. The narrowness of the cold tongue strongly implicates dynamics specific to the equatorial upwelling zone; in most models SSTs slightly off the equator are comparable to (or warmer than) observations. Even in the two models for which the largest (over 2°C) cold bias is found in the equatorial western and central Pacific (EC and UCLA), only a fraction of the error can be attributed to a broader-scale cooling, the rest being due to the westward extension of the cold tongue that plagues almost all the models. Excessive upwelling or stratification errors are the possible dynamical mechanisms for producing a colder than observed minimum SST. The structure and magnitude of equatorial upwelling has been found to be sensitive to the treatment of vertical mixing (Blanke and Delecluse 1993) and even to the horizontal diffusion (Stockdale et al. 1993; Maes, Madec, and Delecluse 1994, personal communication). The MPI and GSFC simulations shown here represent significant improvements over earlier versions, obtained after modifying the mixing parameterizations.

The structure of the cold tongue can be affected by a number of processes, including geographic distribution of the winds (which affects the positions of upwelling, thermocline slope, and zonal currents), insufficient depth of the mixed layer near the warm-pool margin, and excessive upwelling or westward surface current. To a lesser degree, westward extension of the cold tongue has been noted in a number of the ocean model components (Stockdale et al. 1993). However, the variety of shapes of the equatorial SST profile, the large westward extension found in some coupled models, and the differences even between models that share similar OGCM components suggest that the problem does not lie in the ocean component alone, and coupled feedbacks are implicated. The conjecture that the longitudinal structure of the cold tongue and warm pool along the equator is governed to a significant extent by coupled feedbacks between ocean dynamics, the longitudinal SST gradient, and the Walker circulation has been termed "the climatological version of the Bjerknes hypothesis" (Neelin and Dijkstra 1995). Dijkstra and Neelin (1995) examine how this equatorial structure is determined in a simple coupled model and find that it has a strong dependence on model parameters that affect coupled feedbacks. In particular, they note that if the feedback of thermocline slope on SST is

weak or if the ocean model produces a slightly too strong upwelling response to wind stress, the cold tongue tends to extend or shift westward. In the GCMs, of course, a number of other mechanisms can potentially contribute, as discussed below. However, the simple model provides a prototypical example of how a relatively simple error in one process can be turned into a complicated error field by three-dimensional coupled feedbacks.

In the second category, we note that all the models have warmer SSTs over a broad region in the eastern Pacific south of the equator, persisting through all or much of the year. This is generally accompanied by a large eastward extension of the lobe of the western Pacific warm pool that is associated with the southern Pacific atmospheric convergence zone in observations. In the models this warm water is often associated with a double ITCZ with substantial precipitation both north and south of the equator over much of the eastern Pacific most of the year. This suggests that this problem can be considered most simply in terms of annual average conditions, as used in some simpler models. In essence, the GCMs tend to produce a simpler climatology than observed; one that is much more symmetric about the equator. The spatial extent of the warm region suggests that it is not merely a coastal phenomenon, although coastal effects may be important, but must also involve large-scale interactions.

The basic northwest–southeast orientation of the west coast of the Americas is believed to favor a convergence zone north of the equator in the eastern Pacific while discouraging one to the south, and this may determine the mean position of the ITCZ even over the central Pacific (Mitchell and Wallace 1992). The coastal orientation parallels the southeast trades, leading to strong coastal upwelling south of the equator while tending to block the northeast trades. Coupled feedbacks may nevertheless play a vital role. In Xie and Philander (1994) and Xie (1994), simple and hybrid coupled models, respectively, are used to examine cases where coupled interactions produce an asymmetric ITCZ (e.g., north of the equator) even under boundary conditions symmetric about the equator. The evaporation–wind feedback is found to play an important role (Xie 1994), with low wind speeds under the ITCZ contributing to maintaining warm water by low evaporation, while the warm water in turn maintains the ITCZ. Feedbacks between cross-equatorial winds and upwelling can similarly provide symmetry breaking mechanisms (Chang and Philander 1994). The models thus switch from the symmetric double ITCZ configuration to a single ITCZ. Recent work (Philander 1994, personal communication) suggests that feedbacks involving stratus clouds can also contribute to maintaining asymmetry. These simpler models may not provide exact representation of the processes involved in the GCMs but can be taken as a prototype for the importance of coupling to the ITCZ problem. The fact that the models are too symmetric about the equator can be construed as circumstantial evidence for the role of coupled feedbacks in maintaining the asymmetry. The asymmetric ITCZ is apparently not trivial to obtain simply by specifying continental boundary conditions similar to observed but as in the equatorial SST problem discussed above may be strongly affected by coupled feedbacks.

Specific mechanisms that may be associated with the failure to generate sufficient asymmetry in the GCMs include the evaporation–wind feedback, stratus cloud effects, and coastal effects, any of which may be spread or compounded by other feedbacks. The evaporation wind feedback seems to be more important in the MPI integration than the positive feedback between stratus clouds and SST, but here it appears to *maintain* the model's double ITCZ. Thus this feedback can cut both ways. The role of stratus clouds is perceived to be important due to deficiencies in the simulation of PBL stratus decks that are observed to extend long distances off the South American coast (Klein and Hartmann 1993). Indeed all the models overestimate the incident shortwave radiation into the ocean in this region. Once SSTs start to rise, stratus cover may tend to decrease further, leading to a positive feedback on SST. Preliminary experiments by several of the participating groups suggest that the warm bias west of Peru can be substantially reduced by improving the distribution of stratus cloud. Experiments at UCLA, however, indicate that the equatorial cold tongue may become even stronger as the cooling effect is spread northwestward. In addition, work by Miyakoda et al. (1994, personal communication) suggests that prescribing stratus cover alone may not be enough to alleviate the warm bias altogether and that the surface wind distribution is crucial.

Coastal processes may also be important, provided other feedbacks spread the effects into the basin. Underestimated coastal upwelling may contribute to the anomalously warm SSTs off the coast of Peru. This deficiency was also noted in the uncoupled OGCMs analyzed by Stockdale et al. (1993), where insufficient OGCM resolution or underestimated vertical mixing were suggested. Weak coastal upwelling may also be associated with underestimated alongshore surface winds along the Peruvian coast. The reason for these errors is unclear. A likely candidate is poor resolution of the Andes mountains in the AGCM component of all the CGCMs. Notice that this error appears in both gridpoint and spectral AGCMs. It is well known that spectral truncation results in difficulties with sea level values near steep mountains. The simulated low-level winds typically have a substantial unrealistic onshore component in both coupled and uncoupled models. This may be the result of a spurious heat source associated with misrepresenting the Andes as a high-level plateau at the res-

olution of the AGCM. The COLA group has found that extrapolating the surface winds in the interior of the Pacific basin to the South American coastline improves the SST in a narrow band along the coast. In the models whose ocean components are confined to the Tropics, the overestimated temperatures off Peru and Baja California may be associated with poor representation of the midlatitude ocean gyres that advect cold water into these regions. This problem is alleviated somewhat in models that relax to observed temperatures at the north and south boundaries in the subtropics (most models) but may be particularly severe in the NCAR model, which has a zero heat flux boundary condition at all boundaries.

A warm bias off the coast of Peru will tend to be spread northwestward toward the equator by atmosphere and ocean, perhaps contributing to the anomalous eastward extension of a tongue of warm water south of the equator. Once a convergence zone is established south of the equator, it may persist through locally reduced evaporation and mixing (Xie and Philander 1994). The accompanying high convective cloud (low cloud-top temperatures) may also exert a positive feedback on the underlying SSTs. Interestingly, the three models that use the Arakawa–Schubert cumulus parameterization scheme (GSFC, MRI, UCLA: Table 1) all produce a double ITCZ in the eastern Pacific. Of the remaining models, only MPI has a double ITCZ. The MPI model uses a mass flux scheme with a Kuo-type closure (Tiedtke 1989). Our current hypothesis is that the Arakawa–Schubert scheme is more realistically sensitive to overestimated SST, so that convection occurs south of the equator over the eastern Pacific. In the case of the MPI model, it is well known that a CISK-type mechanism can easily give rise to a double ITCZ.

In the third category of common problem for the annual mean, many models—especially CERFACS, GSFC, NCAR—do reproduce the region of SSTs warmer than 29°C that constitutes the western Pacific warm pool. In other models, however, the warm pool is too cool and much too narrow. In the UCLA model, for example, the northeast trades displace too far equatorward in winter, accompanied by large evaporation anomalies suggestive of an evaporative feedback mechanism. The UCLA model uses the Arakawa–Schubert convection scheme, which tends to produce rapidly fluctuating surface wind bursts. These may lead to evaporation being overestimated and account for the overall coldness of this model. Preliminary experiments with a "relaxed" Arakawa–Schubert scheme are underway. No simple model prototype for the latitudinal extent of the warm pool currently exists, but apparently the problem is more complicated than simply a length scale set by the atmospheric radius of deformation for the breadth of warm region.

b. The seasonal cycle

The seasonal cycle in SST peaks in the eastern Pacific in the region where the annual mean SST is most poorly simulated. Nevertheless, four models do obtain a realistic annual cycle in SST in the eastern equatorial Pacific. Interestingly, three of these have the highest AGCM spatial resolution (CERFACS, MPI, and UKMO). In fact, when the horizontal resolution in the AGCM of the MPI model is halved to T21, the simulated seasonal cycle in equatorial SST deteriorates dramatically, with the warm phase of the cycle becoming very weak and the phase error of the cold tongue increasing. It is remarkable that the cold tongue in the eastern Pacific sets in too rapidly in all these models, with the exception of the UKMO model, which seems to have weak eastward propagation rather than the observed westward spread. The rapid onset may be associated with the dominance of local upwelling over other processes. The UCLA simulation is a good example of the very rapid onset of the cold tongue. In this case, equatorial upwelling appears to combine with an elevated thermocline associated with the anomalous southward displacement of the northeast trades (the simulated ITCZ is south of the equator in March) (Robertson et al. 1995a).

The premature appearance of the cold tongue may also be partly associated with deficiencies in the surface heat flux formulation in cases where the semiannual component of the seasonal cold tongue is overestimated (e.g., the MRI simulation). The effect of boundary layer stratus on solar insolation is to enhance the annual cycle in SST, since stratus cover is observed to vary approximately in antiphase with the annual cycle of SST over the eastern equatorial Pacific (Robertson et al. 1995a). Thus, the effect of underestimating the effects of stratus clouds on equatorial solar insolation will be to increase the relative importance of the semiannual harmonic over the annual harmonic. This may shift the onset of the cold tongue farther toward the equatorial minimum in solar insolation at the summer solstice. In the UCLA simulation, however, the annual harmonic is overestimated despite too little stratus cover, so that improving the simulation of the latter may make the seasonal cold tongue even stronger.

Rainfall over the eastern Pacific has a subtle seasonal variation that none of the models is able to reproduce. In the simulations, it either rains on both sides of the equator all year round or rainfall maxima migrate across the equator following the sun. Individual models show these two characteristics to varying degrees. Migration across the equator is most simply explained by insufficient heat capacity in the ocean mixed layer. If the ocean is not able to store enough heat, then the warmest temperatures will strongly tend to follow the solar maximum, and the ITCZ will switch hemispheres. The factors that determine the mixed layer depth involve complex processes since the vertical mixing

schemes employed in the GCMs are sensitive to the heat flux input. Too much heat flux into the ocean tends to shut down mixing, leading to a shallower mixed layer. The migratory behavior may also indicate a lack of the coupled feedbacks discussed above that cause the ITCZ to persist north of the equator and maintain cold SSTs to the south. Models with a double ITCZ appear to primarily underestimate the latter.

c. *Interannual variability*

This work has focused on the simulated seasonal cycle, but the most recent results of the participant modelers are consistent with the apparent lack of correlation between the success in simulating the seasonal cycle and annual mean and obtaining realistic interannual variability of the coupled system. For example, the GSFC model simulates a very realistic spectrum of interannual variability, but its seasonal cycle is poor. In contrast, the CERFACS and UCLA models have quite reasonable seasonal cycles, but interannual variability is weak (Terray et al. 1994; Robertson et al. 1995b). The UKMO model succeeds in simulating quite a realistic seasonal cycle and substantial interannual variability.

d. *Concluding remarks*

All 11 models are able to reproduce the equatorial cold tongue, although it tends to be too strong and too narrow and to extend too far west. Perhaps the most troublesome and widespread systematic error is the overestimation of SST over a broad region west of Peru and in a narrow tongue near 10°S. This is either accompanied by a double ITCZ straddling the equator over the eastern Pacific or an ITCZ that migrates across the equator with the seasons; neither behavior is realistic. The west Pacific warm pool is quite well reproduced by several models but is too narrow in others. There is considerable spread in the quality of the simulated seasonal cycles of equatorial SST in the eastern Pacific. Some models overestimate the amplitude of the semiannual harmonic, while in those with a realistic annual harmonic, the cold tongue tends to appear prematurely.

Despite deficiencies, these results represent major recent advances in model development that are both quantitative and qualitative. Neelin et al. (1992) speculated that coupled feedbacks play important roles in determining the climatology and seasonal cycle in the equatorial Pacific and that such feedbacks could exacerbate model deficiencies. In the meantime, simple models have been able to quantify such feedbacks (Dijkstra and Neelin 1994; Xie and Philander 1994), and their effects have been demonstrated by sensitivity studies using coupled GCMs (e.g., Ma et al. 1994). Improvements in model physics have been magnified by the effects of coupled feedbacks, so that the simulated climatologies presented here have more than fulfilled the expectations of Neelin et al. (1992). We expect this trend to continue. Three years ago, it was unclear how quickly coupled GCMs of the tropical climate would be able to dispense with artificial flux correction to control climate drift, as is often still the case in global coupled models. Since then, careful attention to the physics of air–sea interaction has not only lead to increasing insight into the underlying properties of the coupled system but also to a rapid reduction of climate drift without recourse to artificial flux correction.

Future work needs to proceed in three directions: (i) Deficiencies in the uncoupled component models require further investigation. In the atmosphere, we have drawn attention to the apparent importance of boundary layer stratus cloud for the surface heat budget and the coupled system. In the ocean, we have noted the paradoxical strength of the equatorial cold tongue for generally weak winds. There is a need to examine the performance of contemporary OGCMs when integrated with the same prescribed boundary conditions, as pioneered by Stockdale et al. (1993). (ii) This work has underscored the importance of coupled processes in determining the seasonal cycle in the eastern equatorial Pacific. One method of testing the many conjectures made in this paper would be to carry out unified sensitivity experiments. For example, the responses of a subset of the coupled GCMs to the same prescribed anomaly in stratus cloud might be examined. (iii) As the CGCM integrations become longer, it will be of much interest to investigate in detail the relationship between interannual variability and the seasonal cycle in the models.

Acknowledgments. This intercomparison was compiled at UCLA with support under NOAA Grant NA46GP0244 and DOE-CHAMMP under DE-FG03-91ER61214. We are grateful to K. Arpe for providing the observed OLR data and to G. Cazes for assistance in drafting figures.

REFERENCES

Andrich, P., P. Delecluse, C. Levy, and G. Madec, 1988: A multitasked general circulation model of the ocean. *Science and Engineering on Cray Supercomputers; Proceedings of the Fourth International Symposium,* Cray Research, 407–428.

Barth, N., and J. Polcher, 1994: Two ocean/atmosphere simulations using OPA6 and LMD5bis. Laboratoire de Meteorologie Dynamique, Tech. Rep.

Battisti, D. S., and A. C. Hirst, 1989: Interannual variability in the tropical atmosphere–ocean system: Influence of the basic state and ocean geometry. *J. Atmos. Sci.,* **46,** 1687–1712.

Blanke, B., and P. Delecluse, 1993: Variability of the tropical Atlantic Ocean simulated by a general circulation model with two different mixed layer physics. *J. Phys. Oceanogr.,* **23,** 1363–1388.

Bryan, K., 1969: A numerical method for the study of the circulation of the world ocean. *J. Comput. Phys.,* **4,** 347–376.

Cane, M. A., S. E. Zebiak, and S. C. Dolan, 1986: Experimental forecasts of El Niño. *Nature,* **321,** 827–832.

Chang, P., and S. G. H. Philander, 1994: A coupled ocean–atmosphere instability of relevance to the seasonal cycle. *J. Atmos. Sci.,* **51,** 3627–3648.

Cox, M. D., 1984: A primitive equation three-dimensional model of the ocean. GFDL Ocean Group Tech. Rep. 1, 143 pp.

Dijkstra, H. A., and J. D. Neelin, 1995: Ocean–atmosphere interaction and the tropical climatology. Part II: Why the cold tongue is in the east. *J. Climate,* **8,** 1343–1359.

Gent, P. R., and J. J. Tribbia, 1993: Simulation and predictability in a coupled TOGA model. *J. Climate,* **6,** 1843–1858.

Ineson, S., and M. K. Davey, 1994: Some results from a coupled TOGA model. *Proc. IOC WestPac III Meeting,*

Janowiak, J. E., and P. A. Arkin, 1991: Rainfall variations in the tropics during 1986–1989, as estimated from observations of cloud-top temperature. *J. Geophys. Res.,* **96,** 3359–3373.

Jin, F.-F., J. D. Neelin, and M. Ghil, 1994: El Niño on the devil's staircase: Annual subharmonic steps to chaos. *Science,* **264,** 70–72.

Klein, S. A., and D. L. Hartmann, 1993: The seasonal cycle of low stratiform clouds. *J. Climate,* **6,** 1587–1606.

Latif, M., T. Stockdale, J. Wolff, G. Burgers, E. Maier-Reimer, M. M. Junge, K. Arpe, and L. Bengtsson, 1994a: Climatology and variability in the ECHO coupled GCM. *Tellus,* **46A,** 351–366.

——, T. P. Barnett, M. A. Cane, M. Flügel, N. E. Graham, H. von Storch, J.-S. Xu, and S. E. Zebiak, 1994b: A review of ENSO prediction studies. *Climate Dyn.,* **9,** 167–179.

Ma, C.-C., C. R. Mechoso, A. Arakawa, and J. D. Farrara, 1994: Sensitivity of tropical climate in a coupled ocean–atmosphere general circulation model. *J. Climate,* **7,** 1883–1896.

Mitchell, T. P., and J. M. Wallace, 1992: The annual cycle in equatorial convection and sea surface temperature. *J. Climate,* **5,** 1140–1156.

Nagai, T., T. Tokioka, M. Endoh, and Y. Kitamura, 1992: El Niño–Southern Oscillation simulated in an MRI atmosphere–ocean coupled general circulation model. *J. Climate,* **5,** 1202–1233.

——, Y. Kitamura, M. Endoh, and T. Tokioka, 1995: Coupled atmosphere–ocean model simulations of El Niño–Southern Oscillation with and without an active Indian Ocean. *J. Climate,* **8,** 3–14.

Neelin, J. D., 1991: The slow sea surface temperature mode and the fast-wave limit: Analytic theory for tropical interannual oscillations and experiments in a hybrid coupled model. *J. Atmos. Sci.,* **48,** 584–606.

——, and H. A. Dijkstra, 1995: Ocean–atmosphere interaction and the tropical climatology. Part I: The dangers of flux correction. *J. Climate,* **8,** 1325–1342.

——, and Coauthors, 1992: Tropical air–sea interaction in general circulation models. *Climate Dyn.,* **7,** 73–104.

——, F.-F. Jin, and M. Latif, 1994: Dynamics of coupled ocean–atmosphere models: The tropical problem. *Annu. Rev. Fluid Mech.,* **26,** 617–659.

Oberhuber, J. M., 1988: An atlas based on the COADS data set: The budgets of heat buoyancy and turbulent kinetic energy at the surface of the global ocean. Max-Planck-Institut für Meteorologie Rep. No. 15, 20 pp. plus figs.

Philander, S. G. H., R. C. Pacanowski, N.-C. Lau, and M. J. Nath, 1992: Simulation of ENSO with a global atmospheric GCM coupled to a high-resolution tropical Pacific Ocean GCM. *J. Climate,* **5,** 308–329.

Reynolds, R. W., 1988: A real-time global sea surface temperature analysis. *J. Climate,* **1,** 75–86.

Robertson, A. W., C.-C. Ma, C. R. Mechoso, and M. Ghil, 1995a: Simulation of the tropical Pacific climate with a coupled ocean–atmosphere general circulation model. Part I: The seasonal cycle. *J. Climate,* **8,** 1178–1198.

——, ——, M. Ghil, and C. R. Mechoso, 1995b: Simulation of the tropical Pacific climate with a coupled ocean–atmosphere general circulation model. Part II: Interannual variability. *J. Climate,* **8,** 1199–1216.

Schneider, E. K., and J. L. Kinter III, 1994: An examination of internally generated variability in long climate simulations. *Climate Dyn.,* **10,** 181–204.

Schopf, P. S., and M. J. Suarez, 1988: Vacillations in a coupled ocean–atmosphere model. *J. Atmos. Sci.,* **45,** 549–566.

Stockdale, T., D. Anderson, M. Davey, P. Delecluse, A. Kattenberg, Y. Kitamura, M. Latif, and T. Yamagata, 1993: Intercomparison of tropical ocean GCMs. WRCP-79, WMO/TD-No. 545, 43 pp. plus figs.

——, M. Latif, G. Burgers, and J.-O. Wolff, 1994: Some sensitivities of a coupled ocean–atmosphere GCM. *Tellus,* **46A,** 367–380.

Suarez, M. J., and P. S. Schopf, 1988: A delayed action oscillator for ENSO. *J. Atmos. Sci.,* **45,** 3283–3287.

Terray, L., O. Thual, S. Belamari, M. Deque, P. Dandin, C. Levy, and P. Delecluse, 1994: Climatology and interannual variability simulated by the ARPEGE-OPA model. CERFACS Tech. Rep., TR/CMGC/94–05, 33 pp. plus figs.

Tiedtke, M., 1989: A comprehensive mass flux scheme for cumulus parameterization in large-scale models. *Mon. Wea. Rev.,* **117,** 1779–1800.

Tziperman, E., L. Stone, H. Jarosh, and M. A. Cane, 1994: El Niño chaos: Overlapping of resonances between the seasonal cycle and the Pacific ocean–atmosphere oscillator. *Science,* **264,** 72–74.

Waliser, D. E., and C. Gautier, 1993: A satellite-derived climatology of the ITCZ. *J. Climate.,* **6,** 2162–2174.

Xie, S.-P., 1994: The maintenance of an equatorially asymmetric state in a hybrid coupled GCM. *J. Atmos. Sci.,* **51,** 2602–2612.

——, and S. G. H. Philander, 1994: A coupled ocean–atmosphere model of relevance to the ITCZ in the eastern Pacific. *Tellus,* **46A,** 340–350.

Zebiak, S. E., and M. A. Cane, 1987: A model El Niño southern Oscillation. *Mon. Wea. Rev.,* **115,** 2262–2278.